Shear and Compression Experimental Behaviour of One Leaf Stone Masonry Walls

C. Almeida, J.P. Guedes, A. Arêde
Faculty of Engineering of University of Porto, Department of Civil Engineering

A.G. Costa
University of Aveiro, Department of Civil Engineering

SUMMARY:
Many old buildings located at the Northern part of Portugal, including Porto historical city centre, are made of one leaf stone masonry walls with large and irregular stone blocks. Within the context of the seismic assessment of existing buildings, a masonry wall with those characteristics that was meant to be demolished, was cut into panels and transported to the Laboratory of Earthquake and Structural Engineering (LESE) of the Faculty of Engineering of University of Porto (FEUP) to be tested. The experimental campaign consisted on vertical compression tests on three panels and shear-compression tests on two panels. The compression tests were made first on the walls on their original state and, afterwards, on one of the panels after being injected with lime mortar. This last procedure allowed evaluating the influence of the internal voids found inside the joints in the mechanical properties of the wall (strength and deformability). Finally, shear cyclic in-plane tests for different pre-compression loads were performed to evaluate the walls lateral resistance, energy dissipation capacity and predominant rupture modes. The results obtained with this campaign allowed a first estimation of the mechanical characteristics of such type of stone masonry walls.

Keywords: One leaf stone masonry, Compression tests, Shear compression, Failure modes.

1. INTRODUCTION

Most of the buildings constructed until the beginning of the 20th century at the centre of Porto (classified as world cultural heritage) are made of granite stone masonry walls with timber floors and roofs. In general the buildings are long and narrow, with openings at the front and back facades. The lateral walls, usually made of one leaf of large granite blocks, 30 to 50cm thick, support the timber floor beams and roof trusses.
Not many studies have been taken on walls with such characteristics. In Portugal, experimental tests were carried out in regular one-leaf granite stones built in laboratory environment (Vasconcelos et al, 2009). Tests on double-leaf granite masonry walls built at LESE have also been performed and, in this case, under different strengthening conditions (Costa et al, 2010). Studies carried out in Italy allowed also evaluating, through experimental and in-situ tests, the mechanical properties of multiple-leaf masonry walls (Corradi et al, 2003; Chiostrini et al, 2003).
Recently, a one-leaf granite masonry wall was retrieved from a building located at the centre of Porto to be studied. The wall was part of a building under a renovation project that involved its demolition. The wall was cut into panels and transported to LESE to be submitted to an experimental campaign that included, first, three compression tests and, afterwards, two shear-compression tests. The present work analysis the results obtained in both tests.

2. CHARACTERISTICS OF THE CASE STUDY

The building used as case study was built in 1916 and is located in the centre of Porto, Portugal. The building has a rectangular configuration with an implantation area, of 11.5x30.0m^2. It has an underground floor (floor -1) plus two floors above (floor 0 and floor 1) and a sloped roof. The building is made of granite masonry walls, timber floor beams and roof trusses covered with ceramic tiles. In

average, the masonry consists of medium to large size stones (diagonal length from 50 to 90cm) arranged on regular alignments with a significant number of small stones and, occasionally, pieces of brick (wedges) and mortar joints with variable thickness (0.5 to 2cm), cream colour and brittle behaviour, Figure 1a) (Almeida et al, 2012). Given the characteristics of the structural elements, the building was considered representative of the typical stone masonry buildings found in Porto region.
When this study took place, the building was under a rehabilitation project that included the demolition of a 40 cm thick internal stone masonry wall. Therefore, the wall was cut into panels and transported to the LESE to be tested, Figure 1b) and c). An extensive experimental campaign was then carried out to characterize the mechanical behaviour of the masonry walls and its components. Tests carried out on granite stone samples measured a compressive strength of 60MPa, a modulus of elasticity of 26 GPa and a tensile strength of 3 MPa. The mortar consisted of an air hardening lime with granitic sand on a volume proportion ratio of 1:3 (lime:sand) and aggregate dimensions between 0.25 and 1mm, giving a compressive strength of around 1 MPa. The wall presented large internal voids that were only perceptible by the observation of the cross-section after the cut, Figure 1b).
Uniaxial compression tests were performed on three panels, two in their original state and one after injecting the joints with lime mortar. Interesting results were obtained for the ratio between stiffness (E) and compressive strength (σ_c), which are much different from code standard references or bibliography proposals (Chiostrini et al, 2003; Vintzileou et al, 2007; Valluzzi et al, 2001). Afterwards, two walls were tested under cyclic shear and constant compression force. The results of these tests are presented and discussed in the following sections.

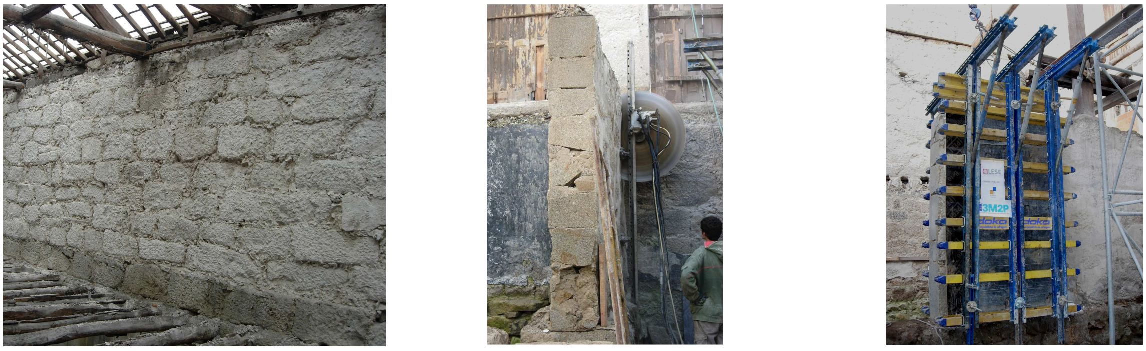

(a) (b) (c)

Figure 1. Building in study: (a) texture of the stone masonry wall; (b) cutting of the wall and (c) confinement system for transporting the wall.

3. COMPRESSION TESTS

3.1. Testing procedure and instrumentation

Uniaxial compression tests were performed in 3 panels identify by PP1, PP2 and PP3. The tests were performed under displacement control, using the 3MN testing machine of the Laboratory for Testing Construction Materials (LEMC) of FEUP. Since the panels were part of a very long wall, i.e. with in situ restricted lateral deformation, they were laterally confined by two steel structures tied together by 2x4 tie rods placed along the wall height and instrumented with load cells (F1 to F4), Figure 2. In order to ensure a good contact between the wall lateral surface and the steel structure, a plastic sleeve was placed in the gap and filled in with grout. Between these sleeves and the lateral steel restrainers, Teflon sheets were inserted in order to reduce tangential contact stresses between the wall and the lateral confinement system.
In order to ensure a uniform distribution of the vertical loads, a very stiff beam made of four HEB200 steel shapes was placed on the top of the wall. The deformations were measured on each wall facade through displacement transducers (LVDTs): two for recording the total vertical deformation (E1, E2), two others for recording a more local vertical deformation (E3, E4) and four to measure the horizontal deformations along the height (T1 to T4), accounting for a total of 16 LVDTs.

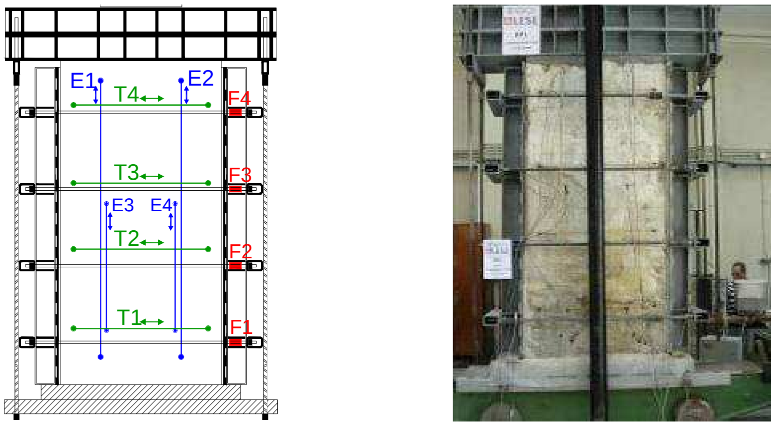

(a) (b)

Figure 2. Compression test setup: (a) general loading and instrumentation scheme and (b) wall being tested.

The PP1 and PP2 panels were compressed monotonically up to a stage considered close to failure and subsequently unloaded. The assumption of failures was made based on the damage state of the panels and conditioned by the risk of a sudden fragile collapse which could put in danger the whole equipment. Afterwards, and in order to check the influence in the results of the wall internal voids found inside the joints, the PP3 panel was tested in two phases. In phase one the wall was compressed with two loading cycles far below the expected strength capacity of the wall. The cycles allowed evaluating the unloading and reloading behaviour, in particular the stiffness of the original wall. Then, in phase two, the joints were injected with grout to fill in the internal voids detected in the walls' cross-section. This operation was done by technicians of a Portuguese external contractor (STAP, S.A.). After 90 days curing, the wall was again tested following the sequence described for PP1 and PP2, but now with intermediate loading cycles.

3.2. Experimental results

3.2.1 Panels PP1 and PP2

The compression tests allowed quantifying deformability parameters and lower bounds of strength for panels PP1 and PP2. Figure 3a) shows vertical and horizontal stress-strain curves. The vertical strain refers to the average values registered by the four vertical longer LVDTs (E1-E2) on the two faces of the walls. Nevertheless, the results are similar to those of the shorter LVDTs (E3-E4). Moreover, the comparison of the results given by the LVDTs on the two façades showed that no significant out-of-plane deformation occurred during the tests.
The analysis of the stress-strain diagrams shows that PP1 and PP2 reached compressive stresses of 3.94 MPa and 2.50 MPa, respectively. Although the curves may point out that a higher strength could have been achieved (in fact, no signs of strength decrease were observed on PP2 curves, and only a light tendency was observed on PP1), the tests were stopped before reaching a clear softening curve branch. As stated above, two reasons enforced this decision: the high level of observed damage already present for those stress levels and the fact that the collapse of these structures is very likely to be sudden and fragile, putting easily in danger the whole testing apparatus. Therefore, the attained values were assumed as a conservative estimate of the compressive strength of the tested panels.
The value of the elastic tangent modulus (calculated at about 30% of the maximum strength) can be determined assuming two types of analysis within the classical theory of elasticity, namely: i) considering the confinement effect (assuming a biaxial plane stress loading conveying an almost plane strain state in the cross-section) or ii) neglecting such effect. The elastic modulus values obtained by these two analyses were comparable, reaching in both cases 0.22 GPa for PP1 and 0.33 GPa for PP2. As a matter of fact, the level of lateral confinement stress introduced in the tests that was only about 6% of the vertical stress at about 30% of the maximum strength, Figure 3a), played a minor role in the evaluation of the elastic modulus. Concerning the ratio between the modulus of elasticity and the compressive strength, there were found values of around 100, thus far below 700, which is the lower bound referred by different authors (Chiostrini et al, 2003; Vintzileou et al, 2007; Valluzzi et al, 2001).

The cracking pattern observed during the tests was essentially vertical, more evident halfway up the wall; the damage became more evident, with local crushing and, mainly, with stones' cracking for a stress level of about 1.5MPa (Figure 3b).

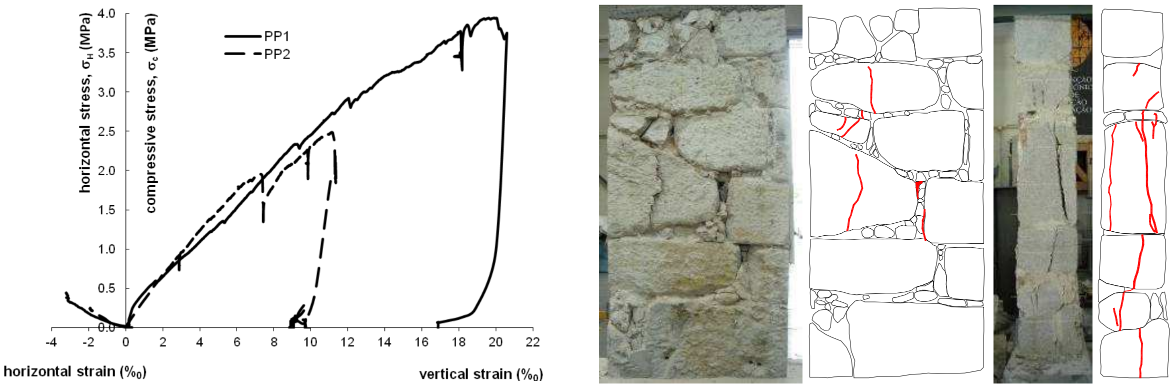

(a) (b)

Figure 3. (a) Vertical and horizontal stress-strain curves for PP1 and PP2 walls and (b) failure lines of PP1 under compression load (front and cross-section views).

3.2.2 Panel PP3

a) Original state

The first test on PP3 focused on the evaluation of the elastic modulus under vertical cyclic loading. In the original state, two loading-unloading cycles were applied to the confined wall: the first cycle up to a stress of 1.0 MPa (about 1/3 of the maximum stress applied to panels PP1 and PP2) and the second up to 1.5 MPa, see Figure 4a).

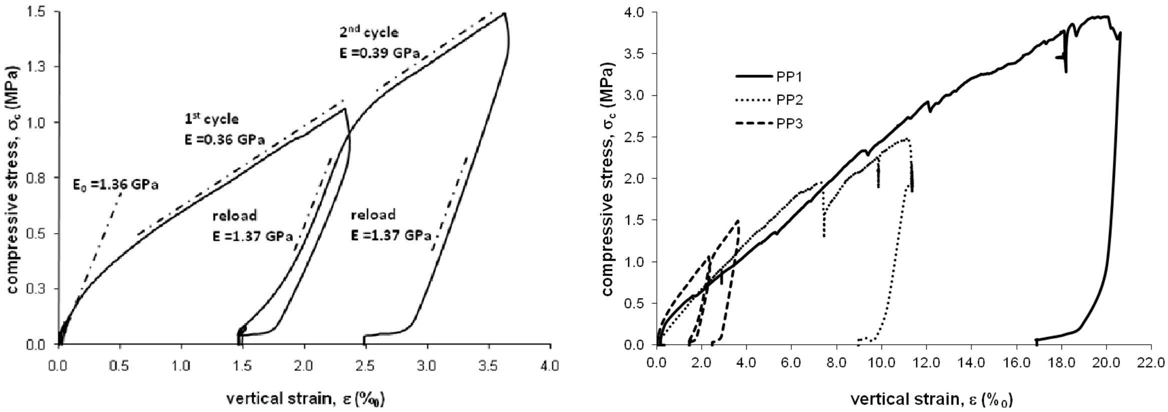

(a) (b)

Figure 4. (a) Axial stress-strain diagrams of the first test on PP3 and (b) comparison of the diagrams between PP1, PP2 and PP3 under the same conditions.

The analysis of the stress-strain diagrams shows different stiffness branches during loading. In an initial state, corresponding to a stress level of about 0.2 MPa, the Young modulus (E_0) was 1.36 GPa. Such stress level is consistent with the load likely to have been applied to the wall during its lifetime; the first branch corresponds to a reloading stage i.e., to a stiffer stress *vs.* strain branch. Once that stress level was overcome, virgin stress states were successively achieved, as exhibited in the first and second cycles, from which low tangent stiffness values were measured, namely 0.36 and 0.39 GPa, respectively. Similar results were observed for PP1 and PP2, Figure 4b). As for the unloading and reloading branches, considerably higher stiffness values are found, about 1.37 GPa, but similar to the initial value (E_0). During unloading, only a small percentage of deformation of the joints' material and contact surfaces is recovered (or recoverable) due to the deformability characteristics of masonry, namely its very high plasticity. At this stage of the test on PP3, no cracking was observed; only a slight detachment of mortar was registered.

b) After injection

In order to assess the influence of the wall internal voids in the panel stiffness, PP3 was then injected with a mortar made of a mixture of air hardening lime, hydraulic lime, sand and water which was meant to have stiffness and strength characteristics close to those of the walls mortar, Figure 5**.**

Figure 5. Injection of mortar in PP3.

After a curing period of 90 days after the injection, PP3 was then submitted to the same loading cycles of the first test: a first cycle up to 1.0 MPa and a second one up to 1.5 MPa, followed by two other cycles at 1.5 MPa. Then, the panel was loaded up to a stress of 2.6 MPa, unloaded and reloaded twice and, finally, it was driven to a stage close to failure, according to the damage level observed on the walls, Figure 6a).

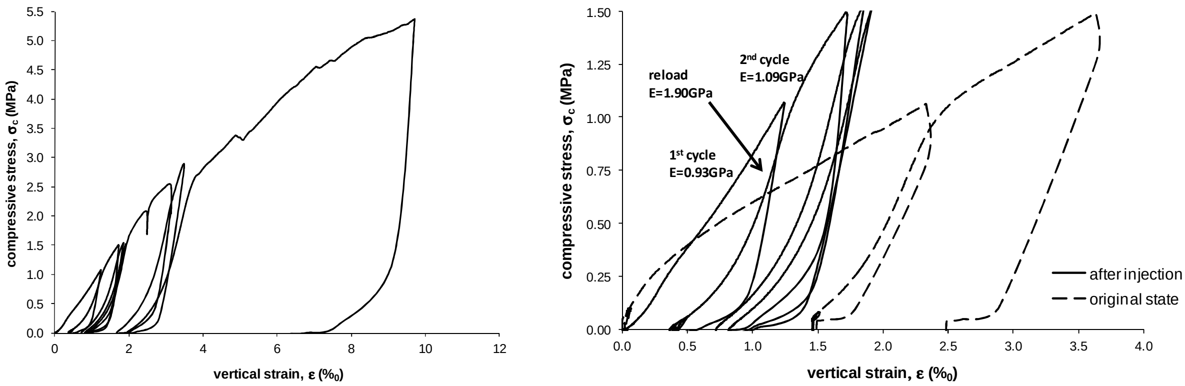

(a) (b)

Figure 6. Results of PP3: (a) compression stress-strain curve after the injection and (b) comparison of the diagrams before and after the injection.

The wall reached a compressive stress of about 5.4 MPa. The test was not driven through the softening range of the response curve for safety reasons. The comparison of this result with the average values obtained for PP1 and PP2 tests shows a strength increase of about 60%. The tangent modulus of elasticity for the first and second loading cycles, reached values of 0.93 GPa and 1.09 GPa, respectively, corresponding to an increase of about 178%, when compared to 0.36 GPa in the original state. In this case, the ratio between the stiffness and the strength corresponds to $E = 185\sigma_c$, a value still far below the one proposed by other authors (Chiostrini et al, 2003; Vintzileou et al, 2007; Valluzzi et al, 2001).

Although the wall had already been subjected to this stress level, the value of the elastic modulus was lower than that recorded during unloading and reloading stages of the original wall (1.37 GPa). Indeed, the injection changed the walls internal properties and the wall got new characteristics. Notice that the walls response curve shows an envelope that is fairly consistent with that of a virgin wall. Concerning the unloading and reloading curves, the results shows stiffness increase leading to Young modulus of 1.90 GPa. Table 1 summarizes the experimental results, where the compressive stress in the original state is the average values measured on PP1 and PP2.

Table 1. Results of compression tests before and after injection.

$(\sigma_c)_{or}$ [a] (MPa)	$(\sigma_c)_{af}$ [a] (MPa)	$(\sigma_c)_{af}$ / $(\sigma_c)_{or}$	E_{or} (GPa)		E_{af} (GPa)		E_{af} / E_{or}	
			1st load	reload	1st load	reload	1st load	reload
3.22	5.40	1.67	0.36	1.37	1.0	1.90	2.78	1.40

[a] Lower limit of compressive strength;
or – original state;
af – after injection.

4. SHEAR COMPRESSION TEST

In-plane shear compression tests aim at evaluating the behaviour of structures under horizontal earthquake type actions, namely assessing their in-plane lateral resistance, energy dissipation capacity and predominant failure modes. In this research, two wall panels identified by PG1 and PG2 were tested. These panels were cut from the same wall of PP1, PP2 and PP3.

4.1. Testing procedure and instrumentation

The apparatus for the shear compression tests consisted on two hydraulic jacks attached to stiff steel reaction frames, in order to impose the vertical and horizontal loads. The vertical load was applied on a steel beam positioned at the top of the specimen in order to ensure a good load distribution, Figure 7a). The specimen was free to rotate at the top. The horizontal displacements were imposed by the horizontal actuator attached the same distribution beam at the top of the specimen; for achieving a correct force distribution and transference along the specimen, transverse steel beams were placed at each end of the wall, connected by steel rods. The specimen was blocked against out-of-plane motion through spherical hinges sliding along two lateral beams.

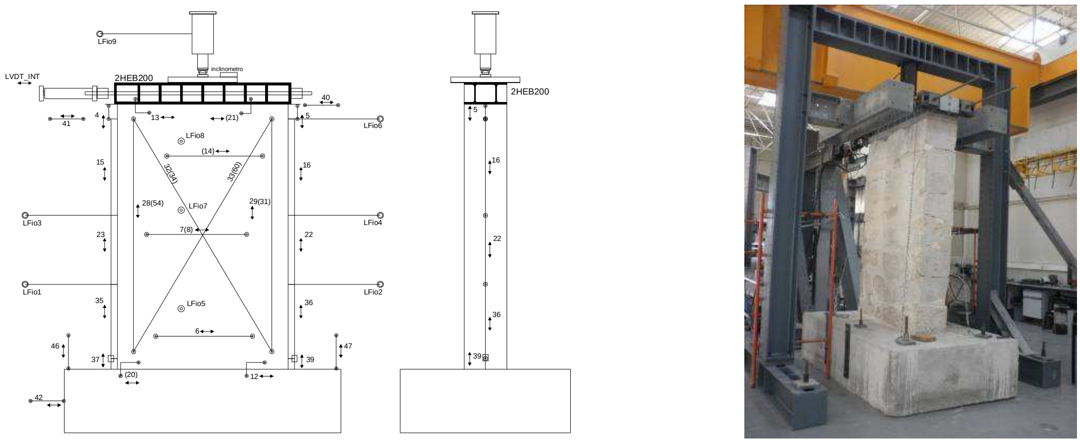

(a) (b)

Figure 7. Shear-compression setup: (a) general loading and instrumentation scheme and (b) wall being tested.

In order to record vertical, horizontal and out-of-plane displacements, the specimens had a complex and dense instrumentation, with a total of 41 LVDTs and one tiltmeter, as illustrated in Figure 7a). The two specimens are 1.6 m long, 2.5 m high and 0.4m thick, corresponding to height/width ratios of about 1.5. The panel PG2 was tested with a constant vertical stress of 0.4 MPa (a value based on the estimated vertical load at the basement of a 5 floors' building, a typology found in many buildings in Porto centre) and PG1 with 0.8 MPa, in order to evaluate the structural response for much higher load levels. Before the main test, and since the vertical force should be applied before any horizontal load, the wall was loaded in the vertical direction following single loading-unloading cycles up to the target vertical stress. This allowed evaluating the compression behaviour, in particular the Young modulus.

Afterwards, the vertical force was kept constant and the shear test started. The test consisted in applying increasing cyclic top displacements (three cycles for each displacement level) until failure.

4.2. Experimental results

4.2.1 Failure mechanisms

Masonry walls subjected to in-plane loading may present three different failure modes which can appear isolated or combined: sliding shear, diagonal shear cracking and flexural. The occurrence of one mode over another depends on several parameters: the panel geometry (texture, cross-section and height/width ratio), the boundary conditions, the vertical load and the mechanical characteristics of their constituents (mortar, blocks and joints) (Tomazevic, 1999). Sometimes, a mixed flexural and shear behaviour occurs.

By assuming the mechanical properties obtained for PG1 and PG2 panels, namely 3MPa for compression strength, 0.03MPa for tensile strength and cohesion (determined through diagonal compression and sliding tests), together with boundary coefficient $\alpha = 1$, shear ratio b = 1.5 and estimated friction coefficient of 0.40, the common expressions found in (Tomazevic, 1999) indicate a the diagonal cracking failure mode. In fact, the failure modes found in the shear tests for PG1 and PG2 were similar. Nevertheless, the final damage in PG1 was more severe than in PG2. In particular, damage started with the detachment of the covering mortar, being followed by mortar joint cracks at the panel mid height due to stones' sliding. Progressively, the cracks extended through mortar joints and stones along the panel height, putting into evidence the failure lines. Once completely formed, these lines separated two volumes of stones, which behaved as independent rigid blocks. The rotation of these blocks lead to compressive stress concentration at the wall base, causing toe crushing, which was found more evident in PG1, due to the higher level of vertical force. Figure 8 illustrates the final state of the two tested panels and Table 2 presents the experimental results from the shear compression tests on PG1 and PG2, including the observed failure modes and the horizontal force capacity.

a) b)

Figure 8. Final state of the specimens: a) PG1 (σ_0 = 0.8MPa) and b) PG2 (σ_0 = 0.4MPa).

Table 2. PG1 and PG2 shear compression test.

Panel	$H_{máx.}$(kN)	Failure mode
PG1	121	diagonal cracking/rocking
PG2	71	diagonal cracking/rocking

Figure 9 represents the lateral deformation of PG2 (which was similar for PG1) for both sides and the different levels of imposed top displacements. Since the beginning of the test, both panels showed a weak connection between stone blocks, leading to the observed discontinuities on the lateral deformation. This fact generated important permanent deformations that increased for higher amplitude displacement levels. Based on the deformation analysis, one could conclude that the areas with higher concentration of damage were located at the mid-height of the panel, confirming the observations made during the test.

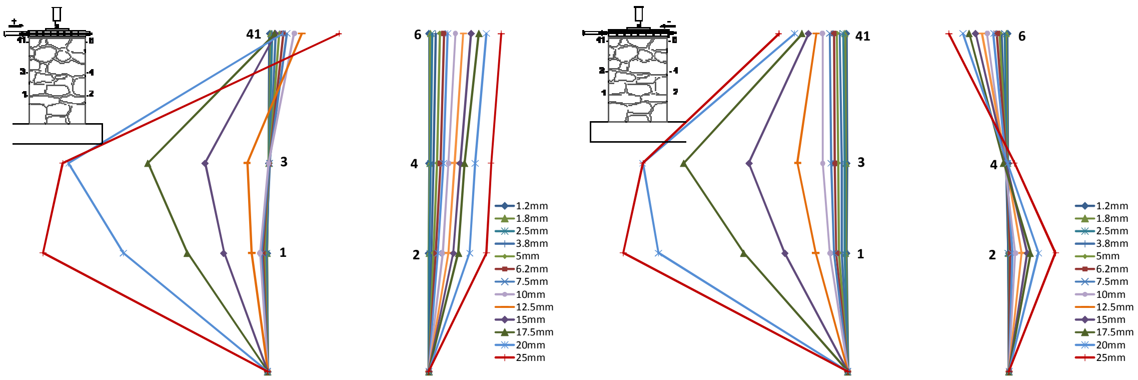

Figure 9. Lateral deformation of PG2 (σ_0 = 0.4MPa).

4.2.2 Lateral resistance and displacement capacity

The hysterical behaviour of a masonry wall under cyclic loading can be represented by an idealized bilinear envelope and, to do so, different procedures are reported in the literature (Tomazevic, 1999; Magenes et al, 1997; Eurocode 8). In general terms, three limited states need to be identified in the horizontal force-displacement curve: the crack limit corresponding to the stage where the first significant cracks (H_{cr}, d_{cr}) appear, the maximum lateral resistance (H_{max}) and the final lateral displacement (d_{max}).

According to the Italian Code (OPCM 3274, 2003), the reference adopted in this analysis, the bilinear curve is obtained by making equal the energy between the experimental envelope curve and the idealized bilinear curve up to the ultimate displacement (d_u), which corresponds to the point where strength degradation is equal to 20% of H_{max}. In some cases, the maximum displacement d_{max} is used instead of d_u, namely when the walls are characterized by a failure rocking mechanism with no significant degradation of the masonry (Vasconcelos et al, 2009).

Both wall panels, PG1 and PG2, were tested for increasing cyclic horizontal displacements up to failure, Figure 10. The stiffness, the maximum lateral force and its degradation were evaluated based on the force-lateral displacement curves and taking the Italian code as reference (OPCM 3274, 2003).

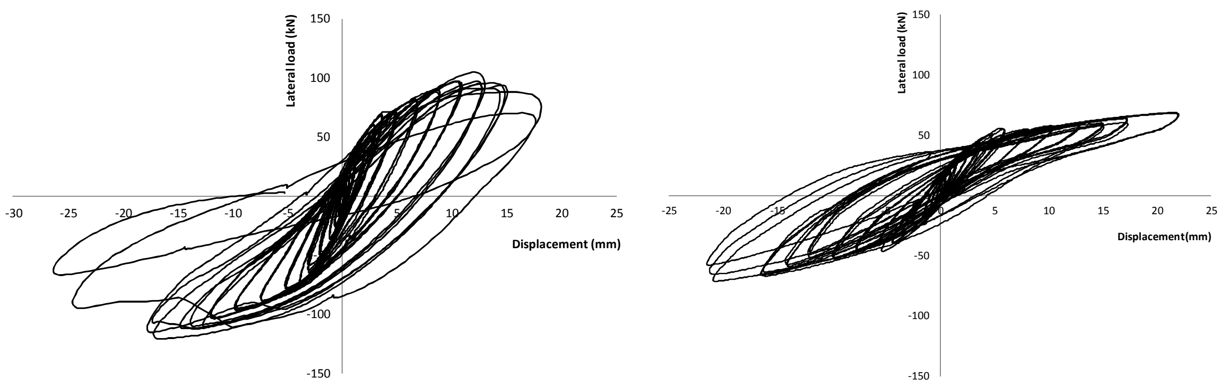

a) b)

Figure 10. Lateral force vs horizontal displacement curves for: a) PG1 (σ_0 = 0.8MPa) and b) PG2 (σ_0 = 0.4MPa).

The shear cracking response is more evident in PG1: pre-cracking response was characterized by moderate hysteresis behaviour and pos-peak with higher energy dissipation and evident strength and stiffness degradation. The PG2 panel showed general moderate hysteresis behaviour, but with lower strength degradation. Moreover, after the pos-peak response the PG2 was governed by rocking response. This behaviour is typical of wall panels with low vertical load when compared to the masonry compressive strength (Tomazevic, 1999).

The envelopes were drawn over the curves in Figure 10 and assuming the contours for the 1st, 2nd and 3rd cycles. Thus, three envelopes were obtained for each direction. Figure 11 shows the results for the 1st cycle. In this analysis, it is assumed that the displacement d_u is equal to the displacement d_{max}, since no significant degradation of load happened in both panels. In conclusion, six envelop and bilinear curves were found for each tested wall panel, which allowed getting a final equivalent bilinear diagram for PG1 and PG2. In particular, the equivalent elastic displacement $d_{e,eq}$ corresponds to the average of the displacements d_e, the equivalent final displacement $d_{u,eq}$ to the minimum value of the displacements d_u and the equivalent lateral force $H_{u,eq}$ to the average of the forces H_u, Figure 12**.** Table 3 summarizes the main results. The elastic stiffness and ductility were obtained by equations (4.1) and (4.2), and the drift by the ratio between the maximum top displacement and the height of the wall.

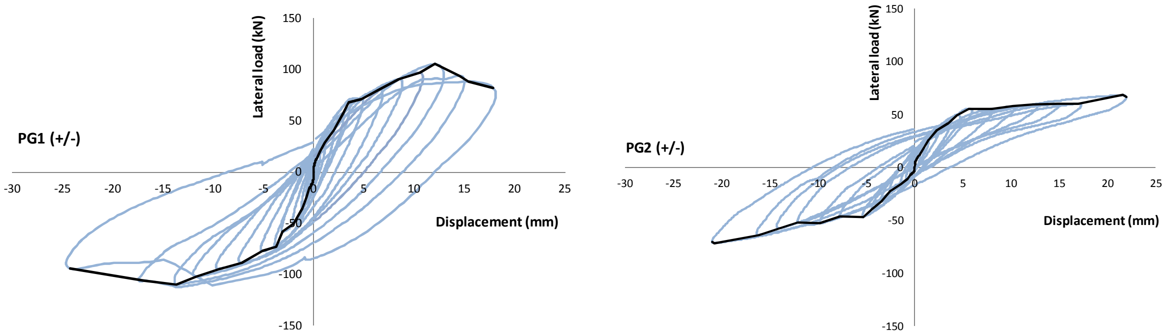

Figure 11. Force-displacement envelops for PG1 and PG2 for the 1st cycle.

$$k_{e,eq} = \frac{H_{u,eq}}{d_{e,eq}} \tag{4.1}$$

$$\mu = \frac{d_{u,eq}}{d_{e,eq}} \tag{4.2}$$

For this wall the ultimate load H_u is around 90% of H_{max}: 91% for the PG1 and 93% for the PG2. This relation fits the proposal by Tomazevic, $H_u = 0.90H_{max}$ (Tomazevic, 1999). The values reached for the secant stiffness (k_e) confirm the clear dependency of the masonry shear behaviour on the installed compression level, as obtained also by other authors, i.e. the increase of k_e with the increase of the compression load σ_0 (Vasconcelos et al, 2009). The identical failure mode observed in both walls led to the same ductility value for PG1 and PG2. Finally, the ultimate lateral drift assumed values in agreement to those pointed out by (Magenes et al, 1997) for brick masonry walls failing in shear.

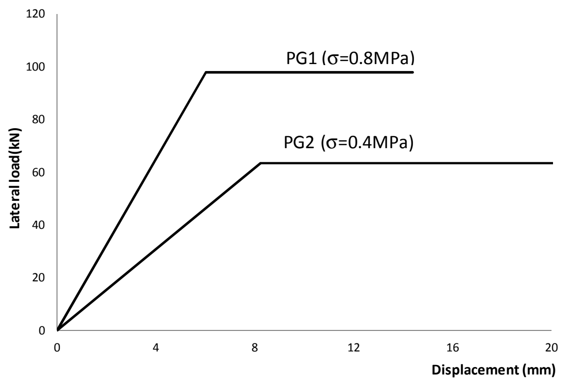

Figure 12. Bilinear diagrams for PG1 (σ_0 = 0.8MPa) and PG2 (σ_0 = 0.4MPa).

Table 3. Values used in the bilinear diagram, for PG1 and PG2.

Panel	H_{cr} (kN)	d_{cr} (mm)	k_e (kN/mm)	d_e (mm)	H_u (kN)	H_{max} (kN)	d_{max} (mm)	Drift (%)	μ
PG1	75.5	4.65	16.26	6.02	97.8	107.8	14.38	0.58	2.39
PG2	47.9	6.16	7.69	8.24	63.3	68.42	20.97	0.84	2.55

5. CONCLUSION

This work aimed at contributing for a better knowledge of one leaf stone masonry walls made of large and irregular stone blocks, a structural element that is present in many buildings of the Northern part of Portugal, including the Porto historical city centre. The available information on this type of walls is still very scarce, demanding more investigation. Nevertheless, this first experimental study using specimens from a real construction allowed assessing the main geometrical and mechanical characteristics of these walls. In particular, it allowed concluding about the low walls' strength, around 3 MPa, and the even lower stiffness, which gives compression stiffness to strength ratios of about 100, thus much lower than the values referred in the general bibliography. Moreover, the improvement of the walls' stiffness and strength capacity after mortar injection allowed concluding that the large amount of voids found inside the joints was partially responsible for the low strength of these walls.
As for the shear-compression behaviour, the walls showed some ductility, around 2.5, and capacity for dissipating energy. The more important damage areas were located in the wall's mid-height, being the failure mode controlled by the formation of two “rigid blocks” separated by a diagonal cracking, which developed mainly through the joints.

AKCNOWLEDGEMENT
The authors acknowledge the collaboration of: the constructor Mota-Engil during the packing operations and transportation of the walls to the laboratory; the constructor STAP, S.A. for the injection operations; architect Adriana Floret; engineer Domingos Martins and the 3M2P constructor for allowing using the building as a case study and for all the support provided during the work, in particular from Mr. Albertino. The contributions of the LESE staff, Mr. Valdemar Luís and André Martins, are gratefully acknowledged. This work includes research carried out with financial support of FCT, through the founding of its research unit CEC (Construction Study Centre of FEUP) and the Ph.D. grant (SFRH-BD-45500-2008) given to the first author.

REFERENCES

Almeida C., Guedes J., Arêde A., Costa C.Q., Costa A. (2012). Physical characterization and compression tests of one leaf stone masonry. Construction and Building Materials; 30: 188-197.

Chiostrini, S. Galano, L., Vignoli, A. (2003). In-Situ Shear and Compression Tests in Ancient Stone Masonry Walls of Tuscany, Italy, Journal of Testing and Evaluation.

Corradi, M., Borri, A., Vignoli, A. (2003). Experimental study on the determination of strength of masonry walls. Construction and Building Materials; 17: 325-337.

Costa A.A., Arêde A., Costa A., Oliveira C. (2010). In situ cyclic tests on existing stone masonry walls and strengthening solutions. Earthquake Engineering and Structural Dynamics 2010; 40:449–471.

Eurocode 8 Design provisions for earthquake resistance of structures. Part 1-1 (1994). General rules and rules for buildings seismic actions and general requirements for structures, ENV 1998-1, CEN, Brussels.

Magenes, G; Calvin G. (1997). In-plane Seismic Response of Brick Masonry Walls. Earthquake Engineering and Structural Dynamics, 26, 1091-1112.

Tomazevic, M (1999). Earthquake-Resistant Design of Masonry Buildings. Imperial College Press, London.

O.P.C.M. n.3274 del 20 Marzo (2003). Primi elementi in materia di criteri generali per la classificazione sismica del territorio nazionale e di normative tecniche per le costruzioni in zona sismica. GU n. 72.

Valluzzi M. R., Porto F. and Modena, C. (2001). Behaviour of multi-leaf stone masonry walls strengthened by different intervention techniques. Historical Constructions, Guimarães, Portugal; 1023-1032.

Vasconcelos G., Lourenço P.B. (2009). Experimental characterization of stone masonry in shear and compression. Construction and Building Materials; 23: 3337-3345.

Vintzileou E., Miltiadou-Fezans A. (2007). Mechanical properties of three-leaf stone masonry grouted with ternary or hydraulic lime-based grouts. Engineering Structures; 30:2265-2276.